Multiline Model for the e-Beam Pumped XeF(B-X) Laser

Tien Tsai Yang,* J. A. Blauer,† C. E. Turner Jr.,‡ and D. A. Copeland†
Rockwell International/Rocketdyne Division, Canoga Park, California

A multivibronic-line, rate-equation model for prediction of e-beam pumped XeF laser performance is described. It self-consistently treats the temporal evolution of the gas and electron temperatures as well as the densities of atomic and molecular species, electrons, and several laser transitions. By correlating species density calculations with observed narrowband absorption data in Ne/Xe plasmas and by invoking certain physical considerations, it is shown that the strong narrowband ($\Delta\lambda \sim 2$ nm) absorption near 351 nm can be reasonably correlated with a neon excimer species. By judicious adjustment of selected rate constants within their range of uncertainty, it has been possible to obtain good agreement with experimental data on pressure- and mix-dependent fluorescence efficiency and also temperature- and wavelength-dependent absorption and small signal gain over a wide range of medium operating conditions. Subsequent predictions of temperature dependent laser efficiency and spectra are found to be in good agreement with available data.

I. Introduction

DUE to their demonstrated high efficiency and potential scalability to large volume and power levels, there has been much recent interest in the rare-gas halide lasers. Among the more efficient of these systems, the xenon fluoride laser exhibits the longest operational wavelength region (351-353 nm), which makes it attractive for several engineering applications of current interest that require good optical beam quality. Since the most judicious path to an understanding of the factors that affect parameter optimization and performance scaling requires a fundamental understanding of the laser medium, much effort has been expended to obtain the needed kinetic and spectroscopic parameters.[1-30] The underlying kinetic mechanism that controls the characteristics of the XeF laser has been discussed briefly by several authors.[1-4] A schematic of the more important energy chains of the proposed pumping mechanism is illustrated in Fig. 1. Once it is formed, the XeF* is subject to two- and three-body quenching by heavy particles and electrons[1,8-12,17] and to collisional interconversion between the B and C electronic states.[9,10,13,19,35,41] It is thought that the operative termolecular quenching processes may involve the formation of triatomic exciplexes.[16] Several radiative processes are also believed to strongly affect the characteristics of this particle laser system. Notable among these are the radiative transitions involving the homo- and heteronuclear rare-gas diatomics (Xe_2*, NeXe*, Ne_2*) and the diatomic and triatomic rare-gas fluorides [NeF*, XeF* (B-X), Xe_2F*, etc.][3,10,11,25,26]

XeF laser oscillation is known to involve several competitive spectral transitions, each with its characteristic bandhead frequency.[20,21,28,31] Previous modeling efforts for this and other similar rare-gas halide laser systems, however, have usually assumed single-line operation in an effort to characterize the gross laser energetics in terms of a single effective transition with homogeneously saturating gain. This approach has limited validity and interpretative difficulties, especially for the bound-bound systems (XeF and XeCl).[1,2,4,32,33,50] Although simple improvements to this approach have permitted some qualitative aspects of spectral mode competition in gain media to be investigated, the quantitative aspects of the problem are relatively untouched.[34] To describe the spectral and thermal characteristics of the XeF laser more realistically, and to gain a more thorough understanding of the associated molecular and laser physics, we have assembled a comprehensive multiline model that describes the transient behavior of e-beam pumped plasmas derived from $Ne/Xe/NF_3/F_2$ mixes.

The model treats the detailed temperature, pressure, and spectral dependence of medium gain, absorption, and laser performance. Excited XeF molecules are assumed to form in high-lying vibrational states by both ionic and neutral particle interactions. The details of the subsequent vibrational relaxation and related B-C state interconversion processes that produce the active lasing states are treated by means of the very compact exponential gap formalism developed by Dreiling et al.[35] for the very similar XeCl system. In applying this model to the XeF molecule, we find only minor parametric adjustments to be necessary.

Theory and experimental data were used in concert to estimate the critical rate parameters and absorption cross sections required by the model. As an example of our approach, we have compared the model predictions to the published medium absorption results of others.[14-16] This comparison permitted the consistent evaluation of the required absorption

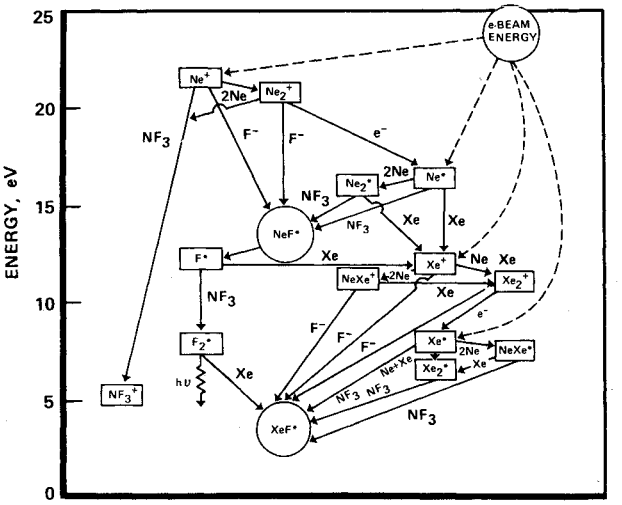

Fig. 1 Major energy channels to upper state laser level of e-beam pumped $Ne/Xe/NF_3$ mixtures.

Presented as Paper 83-1732 at the AIAA 16th Fluid and Plasma Dynamics Conference, Danvers, Mass., July 12-14, 1983; received Nov. 18, 1983; revision received July 27, 1984.

*Member of Technical Staff, Advanced Technology Analysis. Member AIAA.
†Member of Technical Staff, Advanced Technology Analysis.
‡Member of Technical Staff, Special Projects.

cross sections. Similarly, comparisons of the model to fluorescence data[9] permitted a more thorough understanding of certain aspects of the major pumping chains, see Fig. 1. Also, comparisons to published gain data[14] permitted the development of a more consistent model of the vibrational energy exchange within the B-state manifold.

The model has been found to be a very useful tool for mapping the performance characteristics of laboratory and scaled e-beam pumped XeF lasers for both free running and injected operational modes. However, the evolving nature of such models is acknowledged and, indeed, we are continually improving its capabilities. Examples of such improvements already accomplished are the incorporation of a self-consistent Maxwellian secondary electron energy model (not clamped at 1 eV as was typical of earlier models of several groups) and a more realistic model for the pump mechanisms of the lasing states.

In Sec. II, the spectroscopic model, reaction rate model, and energy balance equations are described. Results are discussed in Sec III and a summary is included in Sec. IV.

II. Analytical Model

Spectroscopic Model

Tellinghuisen et al.[28] have accomplished an in-depth analysis of the fluorescence spectra of the XeF molecule and the constants derived are utilized in the model development described herein. The potential energy diagram derived from these and the results of others[9,30,36] is illustrated in Fig. 2.

The gain at line center for individual rotational lines was computed via the form

$$g_c(\omega_c)=\frac{\beta}{8\pi c}\phi_c\frac{S(J',J'')}{\tau\omega_c^2}f(v',J',v'',J'')$$

$$\times\left[\frac{1}{2J'+1}[\mathrm{XeF(B)}]_{v',J'}-\frac{1}{2J''+1}[\mathrm{XeF(X)}]_{v'',J''}\right] \quad (1)$$

where β is the isotopic abendance, $S(J',J'')$ the line strength function,[52] τ the radiative lifetime, and ω_c the frequency at line center. The Franck-Condon factors, $f(v',J',v'',J'')$ are those given in Ref. 28, and the line function ϕ_c is in its pressure limit, i.e.,

$$\phi_c=\sqrt{T}/\pi P a_{\mathrm{Ne}} \quad (2)$$

where a_{Ne} is the half-width half maximum (HWHM) broadening constant.

The gain is averaged over a suitable bandwidth by means of the following term:

$$g(\omega)=\sum_{\ell,J'',m}\left[\int_{\omega}^{\omega+\Delta\omega}\frac{g_c(\ell,J'',m)b_c^2}{(\omega-\omega_c)^2+b_c^2}\mathrm{d}\omega\right] \quad (3)$$

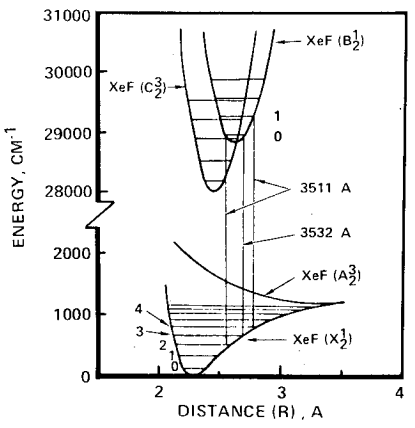

Fig. 2 Schematic of XeF potential energy diagram showing principal laser transitions.

where ℓ is the e and f series (components of doublet), J'' the X-state rotational angular momentum (excluding electron spin), m the P and R branches, $\Delta\omega$ the spectral bandwidth, and b_c the half width at half maximum (HWHM).

The gain is also summed over the contributions of different vibrational transitions where appropriate, and the several isotopes of xenon. A similar approach is used to evaluate the dispersion at high resolution ($\Delta\omega\to 0$). Samples of synthetic gain and dispersion spectra, which are based upon a simple steady-state model,[34] are shown in Fig. 3. With the assumptions of rotational equilibrium and normal homogeneous saturation, the lasing wavelengths are simply the spectral positions of maximum gain within each of the principal transition regions, i.e., in air: $\lambda_1\sim 3511$ Å for (1-4) band, $\lambda_2\sim 3512$ Å for (0-2, 1-4) overlapped bands, and $\lambda_3\sim 3532$ Å for (0-3) band.

Reaction Rate Model

Pumping Reactions for the Upper Laser Level

In electron-beam pumped $Ne/Xe/NF_3$ or $Ne/Xe/F_2$ mixtures, the energy is deposited in the gas principally as electronic excitation and ionization of Ne and Xe. The energy is channeled from these species to the upper laser level of the XeF molecule by means of a series of chemical and physical processes,[38] see Fig. 1.

We have assumed that both the ionic and neutral pumping channels have a branching fraction of unity to the XeF(B) state, i.e., no direct XeF(C) production. This branching assumption is not critical to our model at high pressures where transfer between the B and C reservoirs (Fig. 4) is rapid.[35] However, the actual branching fraction for each formation reaction remains uncertain and, therefore, so does the pressure and mix dependence of the total effective branching to XeF(B,R) and XeF(C,R). For example, the data of Finn et al.[9] suggest a B-state branching fraction in excess of 75% for a special mix at low pressure with e-beam excitation. However, a simple theoretical argument given by Setser[39] suggests values nearer 50% when a photolytic pumping scheme[41] that eliminates the ionic channel is used. In our model, we assume that XeF(C) is formed strictly by collisional quenching or interconversion from the B state.

Vibrational Relaxation

Dreiling et al.[35] have shown that for the similar molecule, XeCl(B,v), the vibrational relaxation rate can be expressed in the form of an exponential energy gap law. For XeCl these authors found that for Ar bath gas, a value for the energy scaling factor $\lambda\sim 0.1$ best fit the data. Using this value of λ, it can be shown that the average energy loss per collision is about

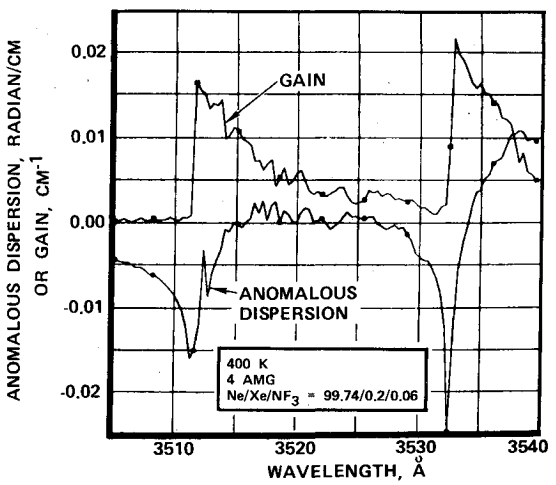

Fig. 3 Sample calculations of anomalous dispersion and corresponding gain spectra.

2200 cm^{-1}, as the XeF* molecule begins the relaxation process near its dissociation limit ($D_0 \sim 43{,}000$ cm^{-1}), where it is assumed to be formed. It requires an average of 20 collisions to reach the bottom of the B-state vibrational energy manifold from which lasing can occur. This assumption is used to estimate the production rate of the lower vibrational levels.

For vibrational relaxation near the bottom of the B- and C-state manifolds, we assume the applicability of a simple energy gap relationship and a rate magnitude similar to that reported for XeCl.[35]

Because of the small concentration of XeF relative to Ne in a typical laser mix, we anticipate that v-v exchanges will, in comparison, be of minor importance.

Collisional Mixing of XeF(B) and XeF(C) States

From state selective laser-induced fluorescence experiments, Fisher et al.[11] have shown that the C-state forms efficiently by collisional quenching of the B state, i.e.,

$$\mathrm{XeF(B},v')+M=\mathrm{XeF(C},v'')+M \tag{4}$$

Brashears et al.[8,41] and others[13,42] have since determined the rate of transfer at low v' as induced by a number of collision partners.

In their analysis of state-to-state relaxation processes in XeCl, Dreiling et al.,[35] found that B-C interconversion collisional transition probability could be expressed in the following form

$$P_{ij}^{T}=\frac{kT}{C}\int_{E_i}^{E_{i+1}}\exp(-C\cdot E^*)\mathrm{d}E^* \tag{5}$$

where i and j specify the quantum levels of the B and C states, respectively. See Ref. 35 for definitions and explanation. Dreiling et al.[35] estimated $C \sim 0.15$ for XeCl relaxation in Ne.

We find a better description of the available data for XeF(B-C) interconversion is obtained for $C_{XeF} \sim 0.10$. Utilizing Eq. (5), we have estimated product distributions for (B-C) interconversions as a function of the initial B-state vibrational energy. The relevant data from which the parametrics of the above model were derived appear in Refs. 8, 10, 12 and 42.

For the (B-C) interconversion of XeCl in Ne, Dreiling et al.[35] show that the rate constants are about five times as efficient at high v as at low v. A simple illustration of these interconversion processes and how they relate to one another is shown in Fig. 4.

In the derivation of rate parameters for individual product channels, we take cognizance of the fact that the C state is thought to be approximately 775 cm^{-1} below the B state.[36] For C-state molecules in their ground vibrational level, this presents a substantial thermal barrier to the formation of the B state. For more highly excited vibrational sublevels of the C state, the reaction endothermicity decreases and the electronic state interconversion becomes more probable.

Collisional Quenching of the Upper Laser Level

An examination of the low lying potential curves illustrated in Fig. 2 reveals three paths for two-body XeF(B) deactivation that are energetically accessible at ambient conditions, i.e.,

$$\mathrm{XeF(B)}+M \rightarrow \begin{cases}\mathrm{XeF(C)}+M & (6a)\\ \mathrm{XeF(A)}+M & (6b)\\ \mathrm{XeF(X)}+M & (6c)\end{cases}$$

Theory[43] and spectral structure seem to indicate that the X state is the most likely terminal state and, since the subsequent decay of the X state to free atoms is rapid, we, as most others, assumed that free atoms are the result. The rate constants for two-body collisional quenching are found in Refs. 8, 10, 11, 12, 41, and 42.

At pressures typical of those existing in laser media (3-5 atm), three-body quenching processes will also be important. Although the products of these termolecular reactions have not been determined, we assume, as in Ref. 32, that they are termolecular exciplexes, Xe_2F^* and NeXeF*. This aspect of our model is based on the considerable data available in the recent literature concerning these processes.[44-46]

Like their B-state analogs, XeF(C) molecules are also efficiently quenched by two-body collisional processes similar to those given by Eq. (6). Our assumption that radiative decay to XeF(X) is a path of minor importance is consistent with the results of Hay et al.[30] For termolecular processes of XeF(C), we assume that the favored products are the termolecular exciplexes, as was assumed for the B state.

Energy Balance

Almost all of the reactions in the model depend upon the temperature of the participating species. Hence, reaction energetics, detailed balance, and energy conservation must be treated systematically to obtain, via self-consistent energy balance, the electron and heavy-particle temperatures that are assumed to be Maxwellian. We will briefly discuss below species and energy conservation equations for both systems.

For the electron gas number density N_e we have

$$\frac{\mathrm{d}N_e}{\mathrm{d}t}=\frac{J}{e}\sum_{\lambda}\sigma_{\lambda}^{+}(E)N_{\lambda}+N_e\left\{\sum_{i}k_iN_i-\sum_{a}k_aN_a\right\}+S_0 \tag{7}$$

where J is the current density, e the electron change, σ_λ the ionization cross section for primary electrons of energy E, λ the index for primary ionization processes, N_λ the number

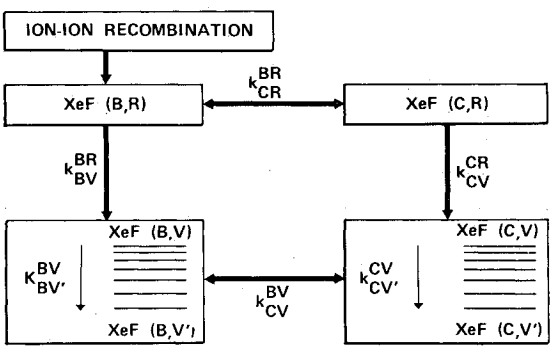

Fig. 4 Interconversion model of XeF(B)↔XeF(C).

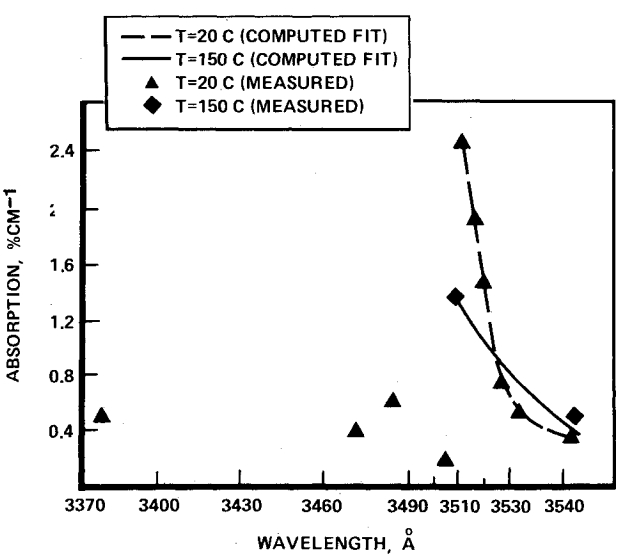

Fig. 5 Absorption in pure neon plasma (experimental data from Ref. 14).

density of molecules of species index λ, k_i and k_a the rate constants for secondary ionization and electron attachment processes, N_i and N_a the number density of ionizing species and attaching species, respectively, and S_0 the formation of electrons by excited state interaction.

The equation that describes the time evolution of the average electron energy $N_e\langle u_e\rangle$ has the following form:

$$\frac{\mathrm{d}}{\mathrm{d}t}N_e\langle u_e\rangle = -\frac{J}{e}\sum_{\lambda} u_{\lambda}^{\mathrm{sec}}\sigma_{\lambda}^{+}(E)N_{\lambda} - N_e(\langle u_e\rangle - \langle u_g\rangle) \times \sum_{m} k_m N_m - N_e\langle u_e\rangle\left(\sum_{s} k_s N_s + \sum_{a} k_a^e N_a\right) \tag{8}$$

where $u_{\lambda}^{\mathrm{sec}}$ is the average energy of the ejected secondary electron for a particular ionization process λ, $\langle u_e\rangle$ and $\langle u_g\rangle$ the mean electron energy and molecular energy, respectively, k_m the rate constant for elastic collisions, k_s the rate constant for electron energy relaxation due to inelastic scattering processes, k_a^e the energy relaxation rate constant for electron attachment processes, and N_s the number density of inelastic scattering species.[51]

The energy equation for heavy particles in e-beam pumped gas at constant density can be expressed in the form

$$P_{\mathrm{beam}} = \sum_i N_i C_i \frac{\mathrm{d}T}{\mathrm{d}t} + \sum_i h_i \frac{\mathrm{d}N_i}{\mathrm{d}t} + \frac{3}{2}k\frac{\mathrm{d}}{\mathrm{d}t}(N_e T_e) + P_s + P_L \tag{9}$$

where P_{beam} is the total power deposition density due to the high-energy electron beam, N_i the molecular density of species i, C_i and h_i the molecular specific heat and enthalpy, respectively, T_e the electron temperature, and k the Boltzmann constant. The spontaneous emission power and lasing power per unit volume are given by P_s and P_L, respectively.

The resulting temperature-dependent rate equations are solved simultaneously with the species equations. This provides a greater degree of accuracy than would be possible if constant temperatures were assumed, especially for high total energy deposition conditions and during beam pump transients.

III. Results and Discussion

Absorption Modeling

The lasing efficiency of e-beam irradiated plasmas produced from Ne/Xe/NF_3 mixtures is known to be affected significantly by the presence of medium absorptions, both broad- and narrowband.[14] Our approach to an understanding of this effect involves the progressive analysis of results pertaining to increasingly complex mixtures. In this view, absorption data for pure neon plasmas were used in tandem with species densities given by model calculations to obtain estimates for the cross sections of the few molecular species known to be present in the medium, i.e., Ne_2^+ and Ne_2^*. Comparisons between the model and absorption data for binary Ne/Xe plasmas were used in the estimation of cross-sectional data for the additional species present therein, i.e., basically $NeXe^+$, Xe_2^+, Xe_2^*, and NeXe*. Similar comparisons for data pertaining to Xe/F_2 and Ne/NF_3 plasmas were used to confirm the results previously obtained and to obtain an estimate for the cross section of F_2^*. Finally, the estimated values of all the cross sections were confirmed by comparisons between the model and absorption data for Ne/Xe/NF_3 and Ne/Xe/F_2 plasmas with potential for XeF(B-X) laser action.

In developing our approach, we recognize the early data-model correlations of Finn et al.,[2] who identified Ne_2^* as the most likely candidate for explanation of the narrowband (351

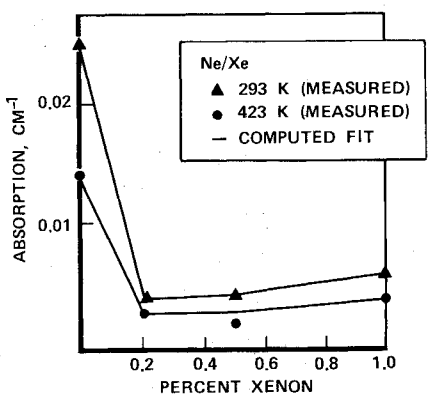

Fig. 6 Computer simulation of absorption in Ne/Xe mixtues at 3511 Å (experimental data from Ref. 14).

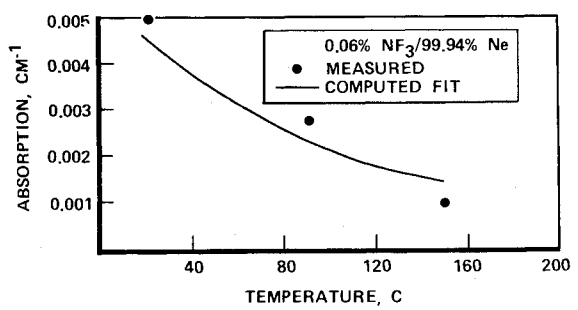

Fig. 8 Computer simulation of absorption in optimum Ne/NF_3 mixtures at 3511 Å (experimental data from Ref. 14).

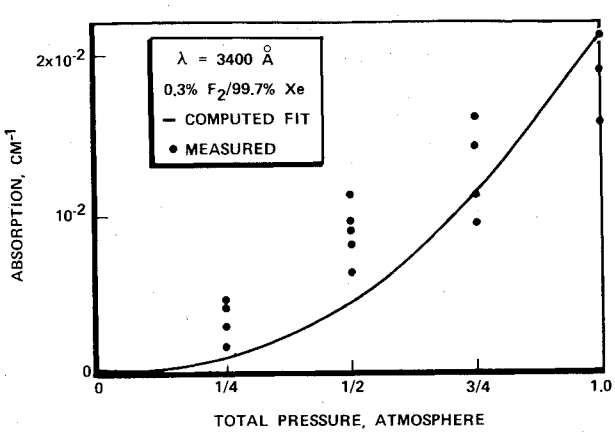

Fig. 7 Absorption comparison for Xe/F_2 mixtures (experimental data from Ref. 16).

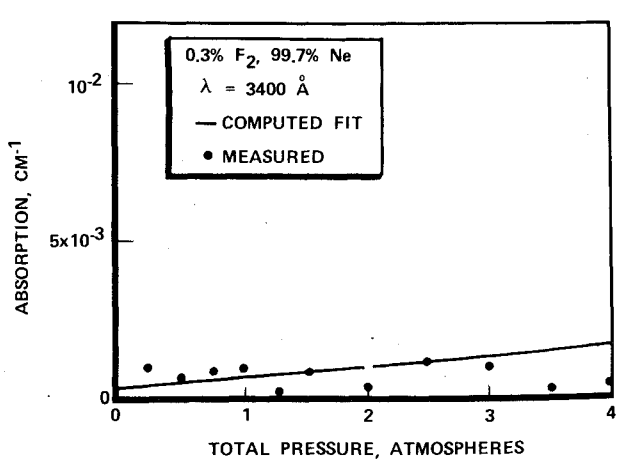

Fig. 9 Absorption comparison for Ne/F_2 mixtues at 3400 Å (experimental data from Ref. 16).

nm) absorption characteristics of Ne-based plasmas. Later Champagne[14] identified a collection of three excited atomic transitions between 351 and 352 nm as the more likely explanation. Although our model, as it is now constituted, could not definitively distinguish between explanations based upon absorptions by Ne* annd Ne_2^*, we note that the absorption bandwidth observed by Champagne[14] for pure Ne plasmas, approximately 20 Å full width half maximum (FWHM), appears inconsistent with the expectations for simple atomic absorptions, see Fig. 5. In this regard, simple collisional or resonance broadening of an atomic line in the spectral region of interest can account for at most only a small fraction of the observed effect (~0.01 Å). Conversely, although other collisional mechanisms (e.g., noncentral collisions) do exhibit broadening widths of the magnitude seen, they are secondary effects of minor magnitude confined principally to the weak wings of a spectral line. These apparent inconsistencies led us to examine Ne_2^* as the principal absorber in the 351-352 nm spectral region for pure neon plasmas.

Typical comparisons between model predictions and published absorption data are found in Figs. 5-9 and Table 1. Predicted species densities for a series of Ne/Xe plasmas are illustrated in Fig. 10. These predictions, when considered in tandem with the corresponding absorption data in Fig. 6, suggest that as Xe is added to the plasma, strong narrowband absorption by Ne_2^* or Ne* is replaced by less absorptive forms, i.e., by $NeXe^+$, Xe_2^+, and Xe_2^*.

A normalized comparison between optical densities observed for Ne/Xe plasmas[14] and the species densities for Ne* and Ne_2^* given by the model when exercised with published rate data[5] is given in Fig. 11. Although this comparison shows a close correspondence between the optical density and the computed Ne* density, it ignores the increasing concentration of Xe-based absorbers as this component is added to the plasma. It is for this reason that the Ne_2^* (O_u^-, $1u$) profile actually gives a better description of the narrowband absorption. We note that a kinetic accounting for the Ne_2^{**} (O_u^+) state is also made in the model formalism. The reason that the Ne_2^* density falls more rapidly than that of Ne* as xenon is added to neon (Fig. 12) is that Penning ionization processes affect both the formation and loss of Ne_2^*. Penning ionization of Xe by Ne* reduces the Ne* concentration and thereby slows the main formation rate of Ne_2^*. The quenching of Ne_2^* is not only through the Penning ionization of xenon but also, more importantly, via dissociative superelastic collisions with secondary electrons whose density is significantly increased by the Penning processes in the Ne/Xe plasmas.

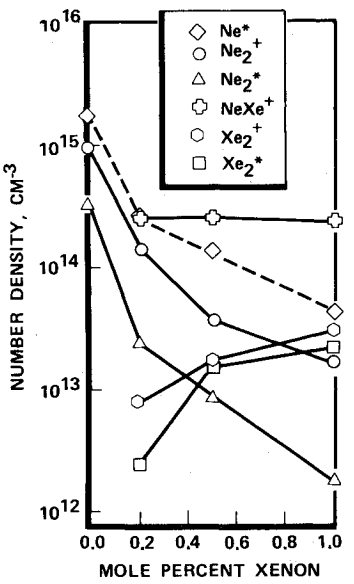

Fig. 10 Computed number densities of major absorbing species in Ne/Xe plasmas at 293 K and 4 Amagat.

Fluorescence

Medium fluorescence yield for the XeF transitions (B→X) and (C→A) has been measured by Finn et al.[9] for laser mixtures of $Ne/Xe/NF_3$ at constant partial pressures of 6 and 2 Torr for Xe and NF_3, respectively. The measurements were taken at 300 K for several neon diluent pressures. The original inverse of the absolute fluorescence yields of B and C of Ref. 9 were combined and converted to total fluorescence efficiency; the results are shown in Fig. 12. The predicted values are included in this figure for comparison. The dependence of fluorescence on neon pressure has been well reproduced.

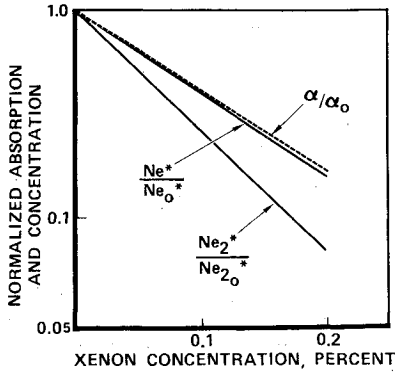

Fig. 11 Correlation of experimental absorption with predicted Ne* and Ne_2^* concentrations.

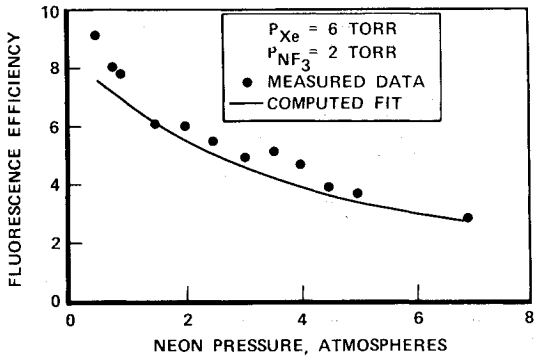

Fig. 12 Fluorescence efficiency comparison (experimental data from Ref. 9).

Table 1 Observed and computed medium absorption for $Ne/Xe/NF_3$ mixtures

Mixture ratio Ne/Xe/NF_3	Density, Amagat	Temperature, K	Absorption, cm^{-1} Experimental	Absorption, cm^{-1} Calculated	Data source
0.9974/0.002/0.006	4	293	0.001 (at 364 nm)	0.0010	NRL[14]
0.993/0.005/0.002	2	300	0.002 (at 340 nm)	0.0009	AVCO[42]
0.993/0.005/0.002	2	450	0.0013 (at 340 nm)	0.0010	AVCO[47]

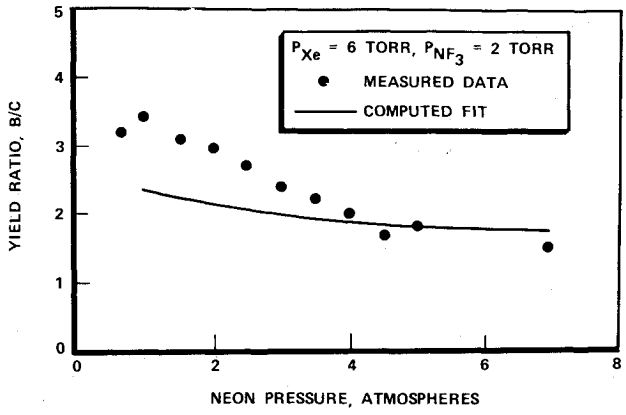

Fig. 13 Comparisons of (B/C) fluoresence ratios (experimental data from Ref. 9).

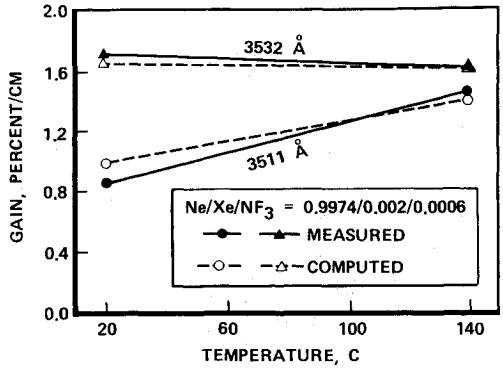

Fig. 14 Computed and measured gain comparisons (experimental data from Ref. 14).

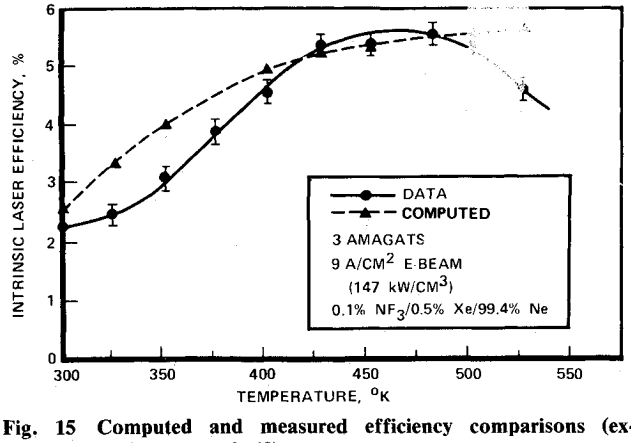

Fig. 15 Computed and measured efficiency comparisons (experimental data from Ref. 48).

Figure 13 shows a comparison of experimental and calculated (B→X)/(C→A) fluorescence yield ratios. At lower pressure, the code underpredicts the ratio, whereas at higher pressure, the calculated B/C ratio agrees fairly well with measured values. The discrepancy of the pressure dependence trend may be due to inadequate treatment of termolecular quenching rates for XeF(C) by 2Ne or Ne + Xe, which have not been well determined experimentally, or to an uncertainty regarding the B/C state branching ratio of the formation step.

Small Signal Gain

The model was further verified by comparison to the available data regarding medium small signal gain,[14] see Fig. 14. The measured gain for $Ne/Xe/NF_3$ mixtures was obtained for an NF_3 composition of 0.06%; a typical concentration for optimum laser performance. Total pressure was 4 Amagat. At room temperature, the measured gain at 3511 Å was 0.0085 cm^{-1} and, as temperature was increased to 423 K, the measured gain increased to 0.0145 cm^{-1}. The measured gain at 3532 Å was 0.017 cm^{-1} at room temperature and 0.016 cm^{-1} at 423 K. The results computed by the code are included in Fig. 14 for comparison. Satisfactory agreement is obtained for a reasonable estimate of experimental uncertainty. Additionally, this comparison substantiates the magnitude of the *V-T* collisional mixing and vibrational relaxation rate constants used in the present analysis.

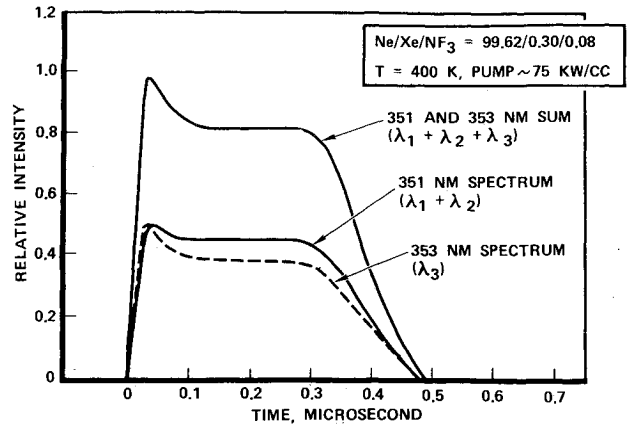

Fig. 16 Experimental time-resolved laser spectrum (experimental data from Ref. 49).

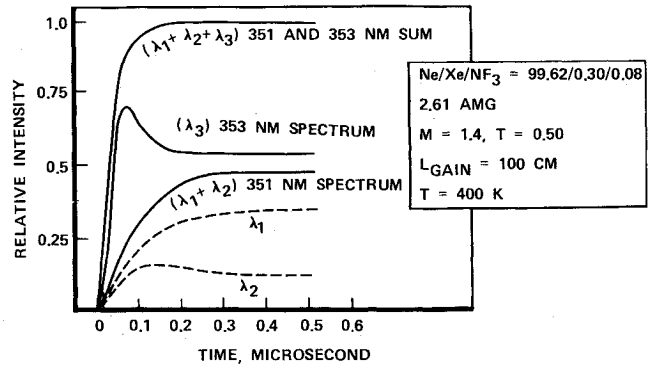

Fig. 17 Time-resolved laser spectrum.

Laser Efficiency

The predictions of the model are in excellent agreement with the measured temperature dependence of laser intrinsic efficiency, as indicated in Fig. 15.[48]

Lasing Spectra

A time-resolved laser spectrum[49] is shown in Fig. 16. The data demonstrate that lasing occurs simultaneously at both 351 and 353 nm throughout most of the pulse duration for the conditions shown. This characteristic is reasonably reproduced by the model prediction as noted in Fig. 17.

IV. Summary

The success of the present model in the various aspects shown above gives reasonable confidence in using its predictions with respect to temperature, wavelength-dependent stimulated emission cross sections, absorption, gain, and laser efficiency in order to interpret available experimental data and to examine the role of various parameters on laser perfor-

mance. We expect this model to be a useful tool for parameteric studies.

Acknowledgments

We would like to thank J. R. Baumgardner and D. M. Smith for their valuable programming assistance and J. J. Vieceli and L. F. Moon for their continued encouragement and support throughout the course of this work. The authors are also grateful to numerous colleagues at many laboratories for enlightening discussions of both published and unpublished research. Special thanks are due to D. L. Heustis and L. J. Palumbo for providing unpublished compliations of reaction data that were a valuable point of departure for this work.

References

[1]Rokni, M., Jacob, J. H., Mangano, J. A., and Brochu, R., "Formation and Quenching of XeF* in Ne/Xe/F_2 Mixtures," *Applied Physics Letters*, Vol. 32, No. 4, 1978, pp. 223-225.

[2]Finn, T. G., Palumbo, L. J., and Champagne, L. F., "Kinetics Scheme for the XeF Laser," *Applied Physics Letters*, Vol. 33, No. 2, 1978, pp. 148-150.

[3]Brau, C. A., "Rare Gas Halogen Excimers," *Topics in Applied Physics*, Springer Verlag, New York, 1979, pp. 87-133.

[4]Huestis, D. L., "The Dominant Kinetic Processes in XeF Laser Media," SRI International, Menlo Park, Calif., unpublished review, 1978.

[5]Heustis, D. L., Hill, R. M., Nakana, H. H., and Lorents, D. C., "Quenching of Ne*, F* and F_2^* in Ne/Xe/NF_3 and Ne/Xe/F_2 Mixtures," *Journal of Chemical Physics*, Vol. 69, No. 11, 1978, pp. 5133-5139.

[6]Flannery, M. R. and Yang, T. P., "Ionic Recombination of Rare Gas X Molecular Ions X_2^+ with F^- in a Dense Gas X," *Applied Physics Letters*, Vol. 32, No. 6, 1978, pp. 356-357.

[7]Flannery, M. R. and Yang, T. P., "Ionic Recombination of Rare Gas Atomic Ions X^+ with F^- in a Dense Gas X," *Applied Physics Letters*, Vol. 32, No. 5, 1978, pp. 327-329.

[8]Brashears, H. C. Jr. and Setser, D. W., "Transfer and Quenching Rate Constants for XeF (II, 1/2) and XeF (II, 3/2)," *Applied Physics Letters*, Vol. 33, No. 9, 1978, pp. 821-823.

[9]Finn, T. G., Palumbo, L. J., and Champagne, L. F., "The Role of the C-State in the XeF Laser," *Applied Physics Letters*, Vol. 34, No. 1, 1978, pp. 52-55.

[10]Waynant, R. W., "XeF(C) State Lifetime and Quenching by Rare Gases and Fluorine Donors," *Applied Physics Letters*, Vol. 36, No. 7, 1980, pp. 493-494.

[11]Fisher, C. H. and Center, R. E., "Radiative Lifetime and Collisional Quenching Kinetics for the XeF (B 1/2) State," *Journal of*

[12]Trainor, D. W., Jacob, J. H., and Rokni, M., "Electron and Heavy Particle Temperature Dependent Quenching Rate Constants of XeF," *Journal of Chemical Physics*, Vol. 72, No. 6, 1979, pp. 3646-3651.

[13]Bischel, W. K., Eckstrom, D. J., Walker, H. C. Jr., and Tilton, R. A., "Photolytically Pumped XeF (C-A) Laser Studies," *Journal of Applied Physics*, Vol. 52, No. 7, 1981, pp. 4429-4434.

[14]Champagne, L. F., "Temperature Dependent Absorption Processes in the XeF Laser," *Applied Physics Letters*, Vol. 35, No. 7, 1979, pp. 516-519.

[15]Champagne, L. F. and Harris, N. W., "The Influence of Diluent Gas on the XeF Laser," *Applied Physics Letters*, Vol. 31, No. 8, 1977, pp. 513-515.

[16]Rokni, M., Jacob, J. H., and Mangano, J. A., "Absorption in Ne- and Ar-Rich XeF Laser Mixtures," *Applied Physics Letters*, Vol. 32, No. 10, 1978, pp. 622-624.

[17]Rokni, M., Jacob, J. H., Mangano, J. A., and Brochu, R., "Two- and Three-Body Quenching of XeF* by Ar and Xe," *Applied Physics Letters*, Vol. 30, No. 9, 1977, pp. 458-460.

[18]Keto, J. W., Gleason, R. E., Bonifield, T. D., and Walters, G. K., "Collisional Mixing of the Lowest Bound Molecular States of Xenon and Argon," *Chemical Physics Letters*, Vol. 42, No. 1, 1976, pp. 125-128.

[19]Rokni, M., Jacob, J. H., Hsia, J. C., and Trainor, D. W., "The Origin of the Broadband Emission in XeF*," *Applied Physics Letters*, Vol. 35, No. 10, 1979, pp. 728-731.

[20]Tanaka, Y., Yoshino, K., and Freeman, D. E., "Emission Spectra of Heteronuclear Diatomic Rare Gas Positive Ions," *Journal of Chemical Physics*, Vol. 62, No. 11, 1975, pp. 4484-4496.

[21]Shimauchi, M., Karasawa, S., and Miura, T., "Spectroscopic Study of a Discharge-Pumped XeF Laser at High Resolution," *Japanese Journal of Applied Physics*, Vol. 17, No. 3, 1978, pp. 527-533.

[22]Velazco, J. E., Kolts, J. H., and Setser, D. W., "Rate Constants and Quenching Mechanisms for the Metastable States of Argon, Krypton, and Xenon," *Journal of Chemical Physics*, Vol. 69, No. 10, 1978, p. 4357.

[23]Oskam, H. J. and Mittelstadt, V. R., "Recombination Coefficient of Molecular Rare-Gas Ions," *Physical Review*, Vol. 132, No. 4, 1963, pp. 1445-1454.

[24]West, W. P., Cook, T. B., Dunning, F. B., Rundel, R. D., and Stebbings, R. F., "Chemiionization Involving Rare Gas Metastable Atoms," *Journal of Chemical Physics*, Vol. 63, No. 3, 1975, pp. 1237-1241.

[25]Burnham, R. and Harris, N. W., "Radiative Lifetime of the B State of XeF," *Journal of Chemical Physics*, Vol. 66, No. 6, 1977, pp. 2742-2743.

[26]Eden, J. G. and Searles, S. K., "XeF (B 1/2) Radiative Lifetime Measurement," *Applied Physics Letters*, Vol. 30, No. 6, 1977, pp. 287-289.

[27]Trainor, D. W., Jacob, J. H., "Electron Dissociative Attachment Rate Constants for F_2 and NF_3 at 300 and 500°K," *Applied Physics Letters*, Vol. 35, No. 12, 1979, pp. 920-922.

[28]Tellinghuisen, P. C., Tellinghuisen, J., Coxon, J. A., Velazco, J. E., and Setser, D. W., "Spectrocopic Studies of Diatomic Noble Gas Halides, IV. Vibrational and Rotational Constants for the X, B, and D States of XeF," *Journal of Chemical Physics*, Vol. 68, No. 11, 1978, p. 5187-5196.

[29]Wadt, W. R., Cartwright, D. C., and Cohen, J. S., "Theoretical Absorption Spectra for Ne_2^+, Ar_2^+, Kr_2^+, and Xe_2^+ in the Near Ultraviolet," *Applied Physics Letters*, Vol. 31, No. 10, 1977, pp.672-674.

[30]Hay, P. J. and Dunning T. H. Jr., "The Covalent and Ionic States of the Xenon Halides," *Journal of Chemical Physics*, Vol. 69, No. 5, 1978, pp. 2209-2220.

[31]Goldhar, J., Dickie, J., Bradley, L. P., and Pleasance, L. D., "Injection Locking of a Xenon Fluoride Laser," *Applied Physics Letters*, Vol. 31, No. 10, 1977, pp. 677-679.

[32]Morgan, W. L. and Szoke, A., "Kinetic Processes in Ar-Kr-F Laser Mixtures," *Physical Review*, Sec. A, Vol. 23, No. 3, 1981, pp. 1256-1265.

[33]Finn, T. G., Chang, R.S.F., Palumbo, L. J. and Champagne, L. F., "Kinetics of the XeCl (B-X) Laser," *Applied Physics Letters*, Vol. 36, No. 10, 1980, pp. 789-791.

[34]Fulghum, S. F. Jr., "XeF Ground State Dissociation and Vibrational Equilibration," Ph.D. Thesis, Massachusetts Institute of Technology, Cambridge, Mass., Feb. 1980.

[35]Dreiling, T. D., and Setser, D. W., "State-to-State Relaxation Processes for XeCl (B,C)," *Journal of Chemical Physics*, Vol. 75, No. 9, 1981, pp. 4360-4378.

[36]Helm, H., Huestis, D. L., and Lorents, D. L., "Laser Induced Fluorescence Studies of XeF (B→X), Paper TuC1, presented at Topical Meeting on Excimer Lasers, Incline Village, Nev., Jan. 1983.

[37]Hazi, A. U., Resigno, T. N., and Orel, A. E., "Theoretical Study of the De-Excitation of KrF and XeF by Low Energy Electrons," *Applied Physics Letters*, Vol. 35, No. 7, 1977, p. 477.

[38]Huestis, D. L., Hill, R. M., Eckstrom, D. J., McCusker, M. V., Lorents, D. C., Nakano, H. H., Perry, B. E., Margevicius, J. A., and Schlotter, N. E., SRI International, Menlo Park, Calif., Rept. MP78-07, May 1978.

[39]Setser, D. W., private communication.

[40]Herzfeld, K. F. and Litovitz, T. A., *Absorption and Dispersion of Ultrasonic Waves*, Academic Press, New York, 1959, pp. 281-282.

[41]Brashears, H. C. and Setser, D. W., "Transfer and Quenchng Rate Constants for XeF(B) and XeF(C) State in Low Vibrational Levels," *Journal of Chemial Physics*, Vol. 76, No. 10, 1982, p. 4932; and *Journal of Physical Chemistry*, Vol. 84, No. 20, 1985, p. 2495.

[42]Gedanken, D. C. and Smith, A. L., "Relative Energies and Collisional Kinetics of the B($\Omega=1/2$ and C($\Omega=3/2$) Excited States of Xenon Fluoride as Studied by Laser-Induced Fluorescence," *Journal of Physical Chemistry*, Vol. 85, No. 19, 1981, pp. 2820-2826.

[43]Dickens, P. G., Linmett, J. W., and Sovers, O., *Transactions of the Faraday Society*, Vol. 58, No. 1, 1962, p. 52.

[44]Eden, J. G. and Waynant, R. W., "Lifetime and Collisional Quenching Measurements of XeF(B) by Photolysis of Xe_2F," *Optics Letters*, Vol. 2, No. 1, 1978, p. 13.

[45]Eden, J. G. and Waynant, R. W., Paper AA5 presented at 30th Annual Gaseous Electronics Conference, Palo Alto, Calif., Oct. 1977.

[46]Eden, J. G. and Waynant, R. W., "Collisional Deactivation Studies of the XeF*(B) State by He, Xe, NF_3 and F_2," *Journal of Chemical Physics*, Vol. 68, No. 6, 1978, p. 2850-2854.

[47]Jacob, J. H. et al., "Investigation of Optimum Laser Pumping," AVCO, Final Tech. Rept., Contract N0014-75-C-0062, Nov. 1979.

[48]Hsia, J. C. et al., "One Meter KrF Laser System," AVCO, Semiannual Rept., Contract N0014-75-C-0062, Nov. 1979.

[49]Tillotson, J. H., Truesdell, K. A., Burde, D. H., Harris, D. G., and Axworthy, A. E., Rocketdyne, unpublished data.

[50]Levin, L. A., Moody, S. E., Klosterman, E. L., Center, R. E., and Ewing, J. J., "Kinetic Model for Long-Pulse XeCl Laser Performance," *IEEE Journal of Quantum Electronics*, Vol. QE-17, No. 12, 1981, pp. 2282-2289.

[51]Johnson, T. H., Palumbo, L. J., and Hunter, A. M. II, "Kinetics Simulation of High Power Gas Lasers," *IEEE Journal of Quantum Electronics*, Vol. QE-15, No. 5, 1979, p. 289.

[52]Herzberg, G., *Spectra of Diatomic Molecules*, Van Nostrand Reinhold Co., New York, 1950, pp. 207-208.